Search for Light Pseudoscalar Boson in the Composite Higgs Model using the CMS Detector

Nicholas Bower[1], Maxwell Chertok[2], John Gunion[2], Redwan Habibullah[1],
Grace Haza[2], **Meutia Nursanto**[1], Rachel Yohay[1],
Fengwangdong Zhang[2], **Jingyu Zhang**[1]

[1]Florida State University
[2]University of California, Davis

2021 Meeting of the Division of Particles and Fields of the American Physical Society (DPF21)

Introduction

- Search for direct light pseudo-scalar production
  → Timid Composite Pseudoscalar (TCP)
- Current bounds come from di-photon searches at masses above 65 GeV and di-muon searches at masses below 14 GeV
- At mass region in between 14 GeV and 65 GeV, the bounds are not competitive
- An opportunity is open to try new strategies that can improve the bounds in this mass range

Motivated by
"Revealing timid pseudo-scalars with taus at the LHC"
(arXiv:1710.11142)

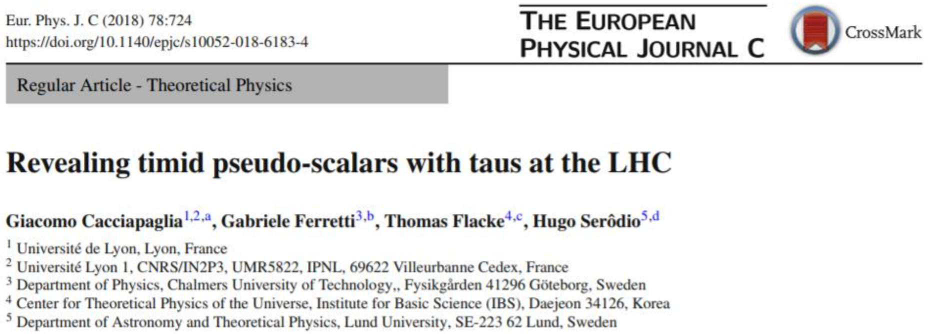
Eur. Phys. J. C (2018) 78:724
https://doi.org/10.1140/epjc/s10052-018-6183-4
THE EUROPEAN PHYSICAL JOURNAL C
CrossMark
Regular Article - Theoretical Physics

Revealing timid pseudo-scalars with taus at the LHC

Giacomo Cacciapaglia[1,2,a], Gabriele Ferretti[3,b], Thomas Flacke[4,c], Hugo Serôdio[5,d]
[1] Université de Lyon, Lyon, France
[2] Université Lyon 1, CNRS/IN2P3, UMR5822, IPNL, 69622 Villeurbanne Cedex, France
[3] Department of Physics, Chalmers University of Technology,, Fysikgården 41296 Göteborg, Sweden
[4] Center for Theoretical Physics of the Universe, Institute for Basic Science (IBS), Daejeon 34126, Korea
[5] Department of Astronomy and Theoretical Physics, Lund University, SE-223 62 Lund, Sweden

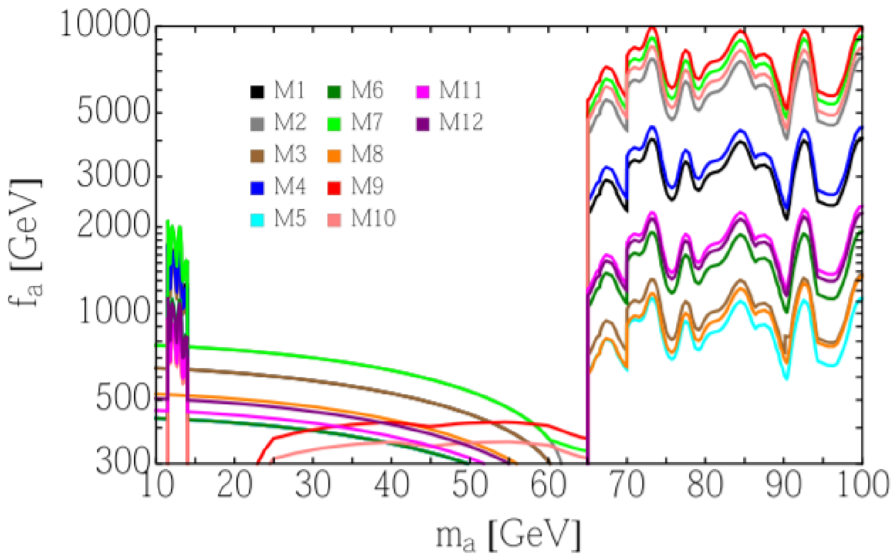

Bounds on the decay constant f_a as a function of pseudo-scalar masses m_a for twelve different models

Introduction

- Dominant decay channels are gg and $b\bar{b}$, both with very large irreducible QCD background
  - Next most frequent: $\tau^+\tau^-$

- A promising topology is that of a boosted TCP recoiling against an ISR jet and then decaying into $\tau^+\tau^-$

- Small separation angles between the $\tau^+\tau^-$ decay products are expected due to the boosting

- All decay modes of the di-tau system can be considered
  i.e. fully leptonic, semi leptonic, fully hadronic

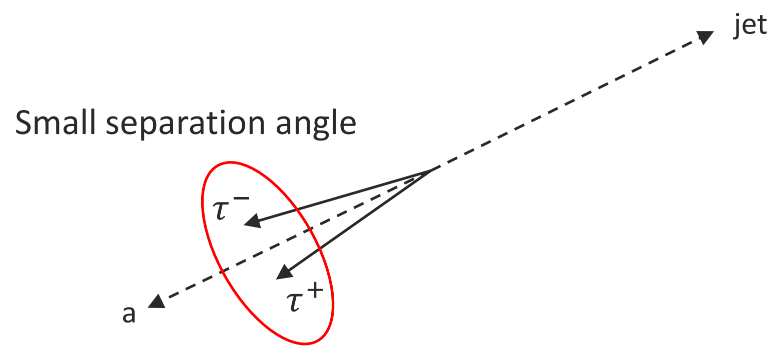

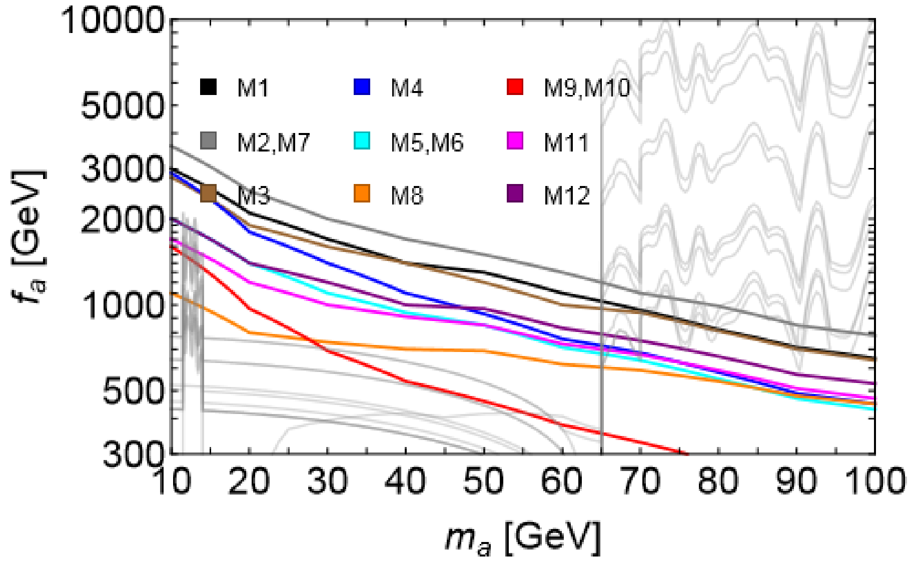

Projection on the bounds on f_a for the various models after an integrated luminosity of 300 fb^{-1} with $\tau_e\tau_\mu$ decay channel

Boosted Di-tau Search

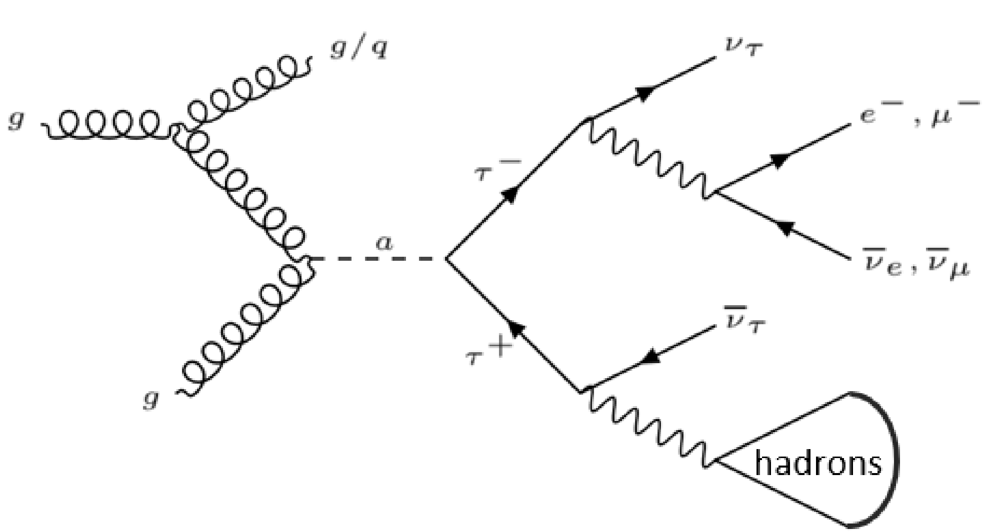

Six possible final states	
$\tau_e\tau_e$	Fully leptonic
$\tau_\mu\tau_\mu$	
$\tau_e\tau_\mu$	
$\tau_e\tau_h$	Semi-leptonic
$\tau_\mu\tau_h$	
$\tau_h\tau_h$	Fully hadronic

- Boosted TCP recoiling against an ISR jet and then decaying into $\tau^+\tau^-$
  → Final state: 2 tau + 1 jet → 6 possible final states
- Largest background come from Drell-Yan and QCD
  - Data-driven method is used to estimate the QCD background in signal region
- Signal samples have been generated at LO for m_a = 10, 30, 50 GeV with a cut at HT-400
- In this presentation $\tau_\mu\tau_\mu$,$\tau_e\tau_\mu$, and $\tau_h\tau_h$ have been investigated

Event Selection

Trigger

Events triggered by Single Muon or Single Jet Triggers.

Muon $P_T > 24$ GeV or $P_T > 50$ GeV, Jet $P_T > 500$ GeV

Object Selection

Muons	Electrons	Taus	Jets
$P_T > 3$ GeV	$P_T > 7$ GeV	$P_T > 20$ GeV	$P_T > 20$ GeV
$\|\eta\| < 2.4$	$\|\eta\| < 2.5$	$\|\eta\| < 2.3$	$\|\eta\| < 2.5$
Isolated	Isolated	Isolated	

Opposite Charge Lepton Pair

ΔR between leptons < 0.4, ΔR between leptons and jet > 0.8

MET > 100 GeV

Fully leptonic	Fully hadronic
$\Delta\phi$ between MET and jet > 2 $\Delta\phi$ between MET and lepton < 1	Veto on isolated muons and isolated electrons

QCD Background Estimation in $\tau_h\tau_h$

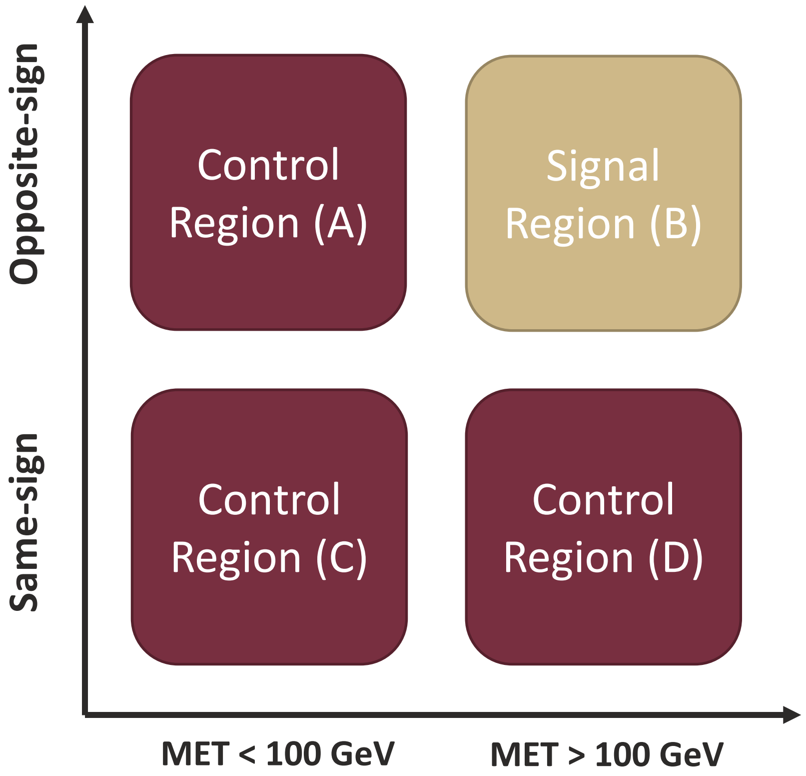

$$\frac{A}{C} = \frac{B}{D}$$

$$N_{(QCD)B} = \frac{N_{(data)A} - N_{(MC)A}}{N_{(data)C} - N_{(MC)c}} \times \left(N_{(data)D} - N_{(MC)D}\right)$$

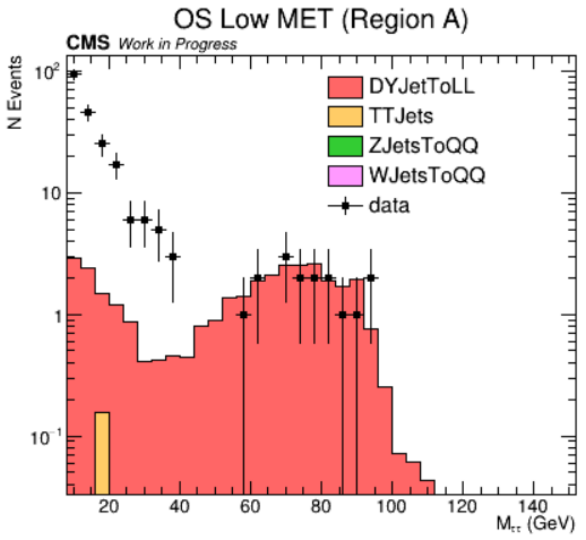

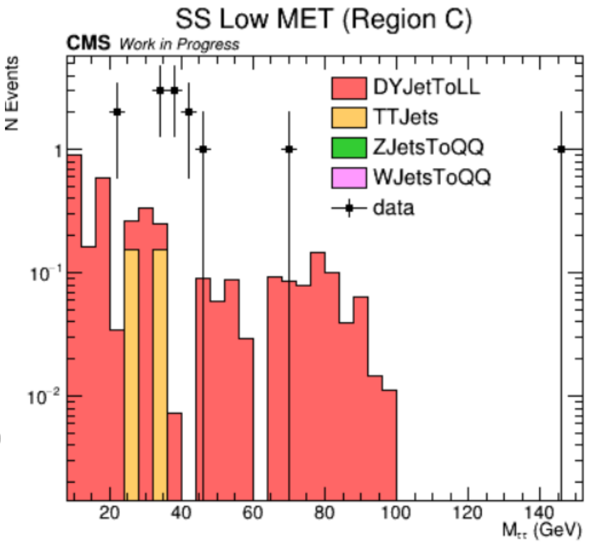

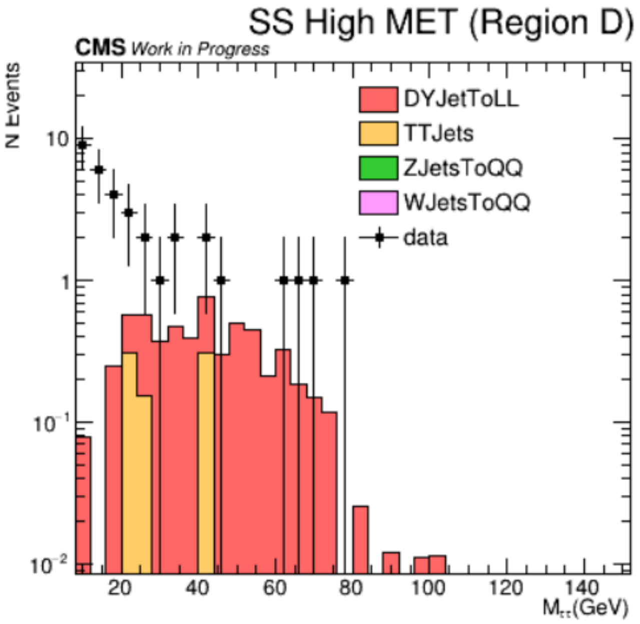

Preliminary Results

Visible mass plots on $\tau_e\tau_\mu$, $\tau_\mu\tau_\mu$, and $\tau_h\tau_h$ final states

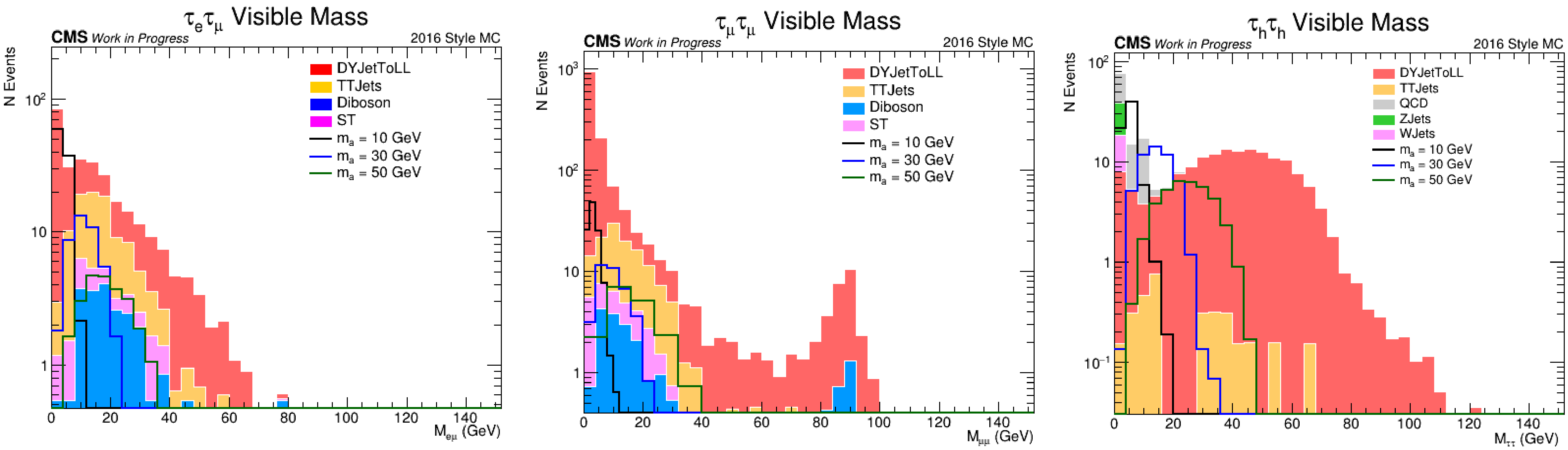

Expected Limits on Decay Constant f_a

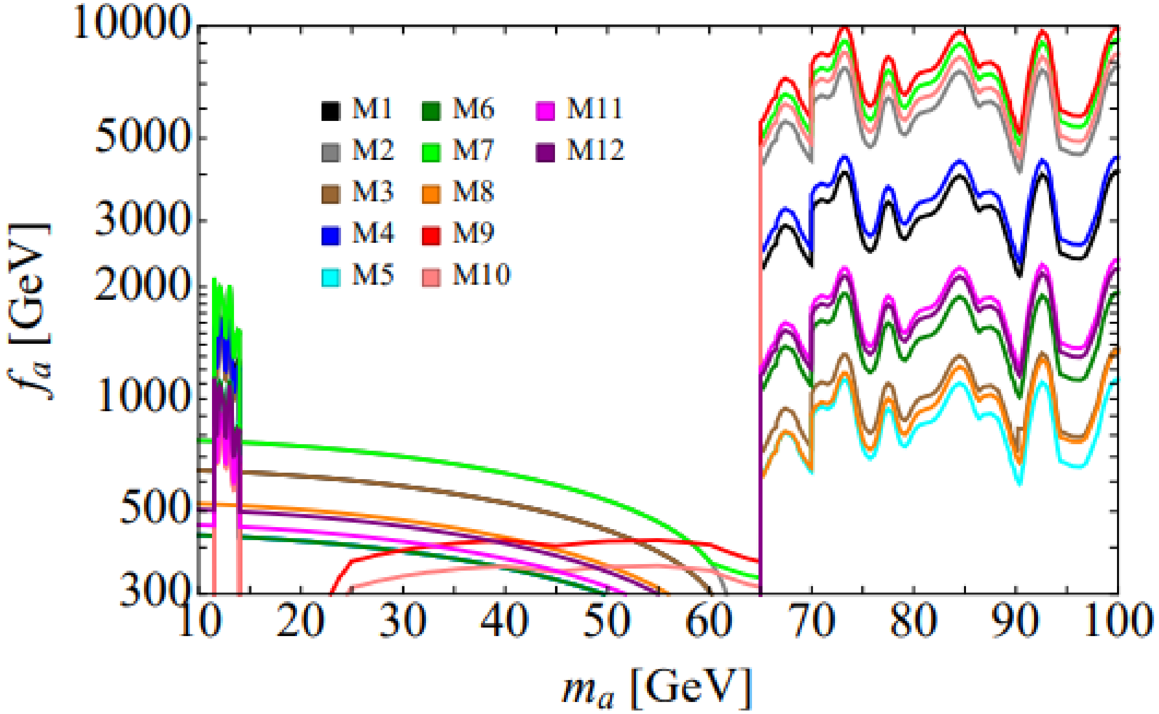

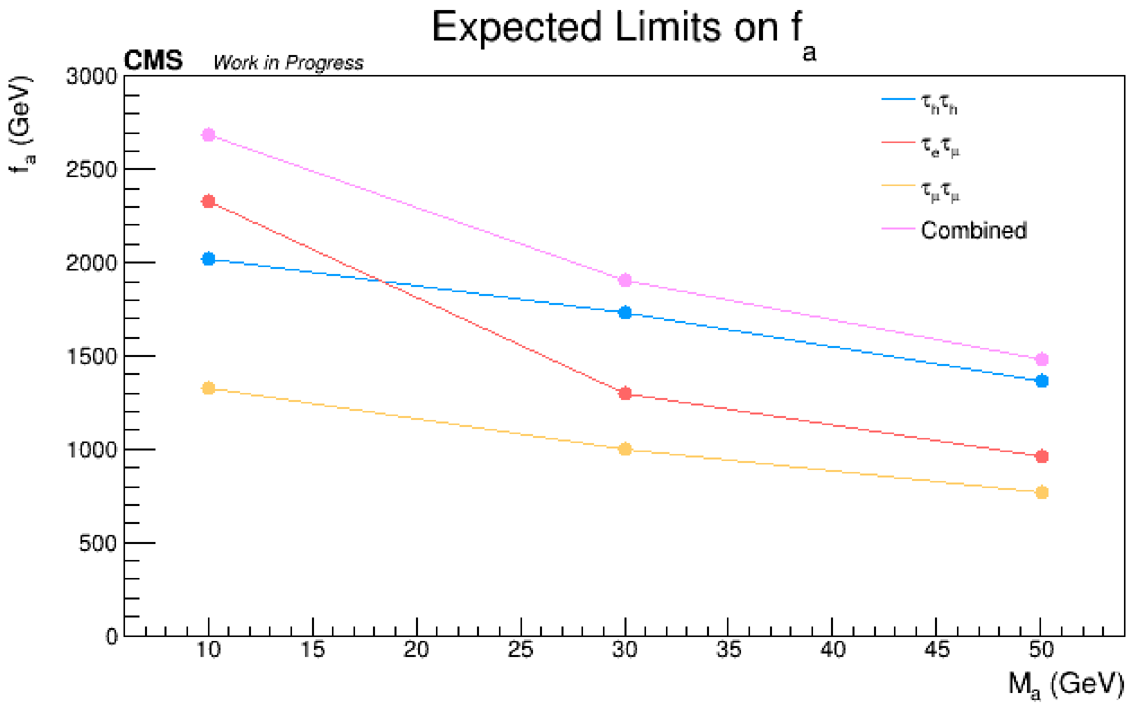

Caveats:

All uncertainties are statistical → No systematic uncertainties have been considered yet

Conclusions and Plans

- Preliminary results on three final states of the TCP shows that the search is accessible in Run 2 and limits on f_a looks promising
- All six final states will be considered
- Estimation methods for other backgrounds will be determined

Backups

Description of the Models

$$\mathcal{L} = \frac{1}{2}(\partial_\mu a)(\partial^\mu a) - \frac{1}{2}m_a^2 a^2 - \sum_f \frac{iC_f m_f}{f_a} a\bar{\Psi}_f \gamma^5 \Psi_f + \frac{g_s^2 K_g a}{16\pi^2 f_a} G^a_{\mu\nu}\tilde{G}^{a\mu\nu} + \frac{g_s^2 K_W a}{16\pi^2 f_a} W^i_{\mu\nu}\widetilde{W}^{i\mu\nu} + \frac{g'^2 K_B a}{16\pi^2 f_a} B_{\mu\nu}\tilde{B}^{\mu\nu}$$

	M1	M2	M3	M4	M5	M6	M7	M8	M9	M10	M11	M12
K_g	-7.2	-8.7	-6.3	-11.	-4.9	-4.9	-8.7	-1.6	-10.	-9.4	-3.3	-4.1
K_W	7.6	12.	8.7	12.	3.6	4.4	13.	1.9	5.6	5.6	3.3	4.6
K_B	2.8	5.9	-8.2	-17.	.40	1.1	7.3	-2.3	-22.	-19.	-5.5	-6.3
C_f	2.2	2.6	2.2	1.5	1.5	1.5	2.6	1.9	.70	.70	1.7	1.8
$\frac{f_a}{f_\psi}$	2.1	2.4	2.8	2.0	1.4	1.4	2.4	2.8	1.2	1.5	3.1	2.6

Signal Generation and Cross Section Re-scaling

Signal generated for $m_a = 10, 30, 50$ GeV, $f_a = 1$ TeV with a cut at HT-400 (2016 styl

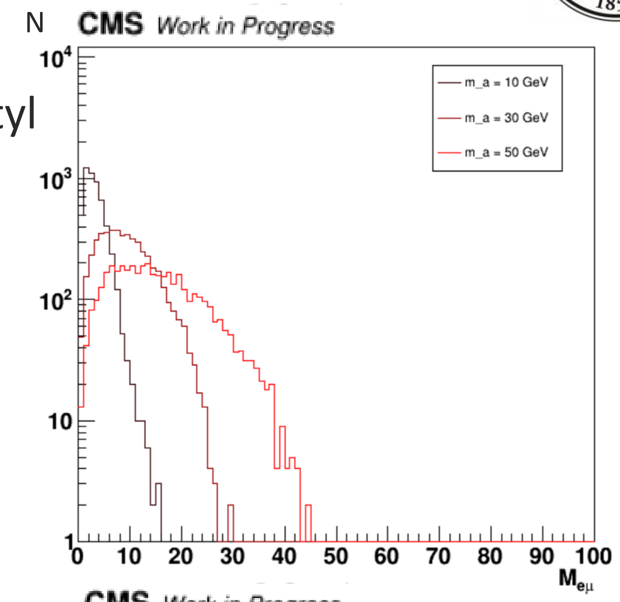

From Madgraph (with the parameters set to be = 1) →

$$\frac{\sigma(ggF \to TCP \to \tau\tau)}{Br_{\tau\tau}} = \sigma(ggF \to TCP)$$

$$Br_{\tau\tau} = \frac{\Gamma_{\tau\tau}}{\Gamma(total)}, \quad \Gamma(total) = 1\ GeV$$

The true value of $\sigma_{\text{prod.}} \times \text{BR}_{\tau\tau} \times \epsilon$ displayed in Table 2 for each model is obtained by multiplying $\bar{\sigma}_{\text{prod.}} \times \epsilon$ by $K^2_{g,\text{eff}} \times \text{BR}_{\tau\tau}$ shown in Table 5. We do not include a k-factor for this analysis. The efficiencies of the cuts depend

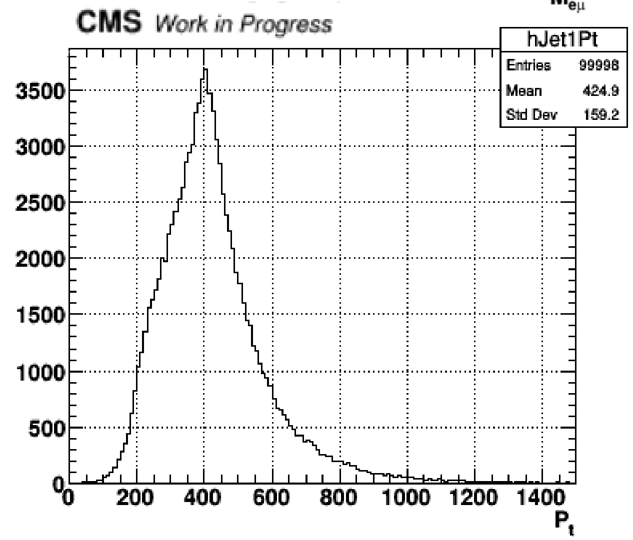

For each model:

$$\sigma(ggF \to TCP \to \tau\tau) = \sigma(ggF \to TCP) \times \kappa^2_{g,eff} \times Br_{\tau\tau}$$

In this talk, we will consider Model 1, $m_a = 10$ GeV

B. Details of the Simulation, pg. 8

$K_{g,eff}^2 \times BR_{\tau\tau}$

m_a [GeV]	10	20	30	40	50	60	70	80	90	100
M1	6.7	3.4	2.5	1.9	1.5	1.2	0.95	0.79	0.66	0.57
M2	9.7	4.8	3.6	2.7	2.1	1.7	1.4	1.1	0.96	0.82
M3	5.7	2.9	2.2	1.8	1.4	1.1	0.91	0.76	0.65	0.56
M4	6.2	2.6	1.6	1.1	0.79	0.60	0.47	0.39	0.32	0.27
M5	3.0	1.5	1.1	0.84	0.66	0.52	0.42	0.35	0.30	0.25
M6	3.0	1.5	1.1	0.84	0.66	0.52	0.42	0.35	0.30	0.25
M7	9.7	4.8	3.6	2.7	2.1	1.7	1.4	1.1	0.96	0.82
M8	0.88	0.50	0.48	0.46	0.43	0.40	0.36	0.33	0.30	0.28
M9	1.9	0.74	0.42	0.27	0.19	0.14	0.11	0.091	0.076	0.064
M10	1.8	0.73	0.41	0.27	0.19	0.14	0.11	0.091	0.076	0.064
M11	2.1	1.1	0.94	0.79	0.66	0.55	0.47	0.40	0.35	0.30
M12	2.9	1.5	1.3	1.0	0.85	0.70	0.59	0.50	0.43	0.37

Background Processes

Physics process	Dataset name	σ (pb)
Z/γ^*	DYJetsToLL_M-1To5_HT-150to200_TuneCUETP8M1_13TeV-madgraphMLM-pythia8	1124.0
	DYJetsToLL_M-1To5_HT-200to400_TuneCUETP8M1_13TeV-madgraphMLM-pythia8	789.8
	DYJetsToLL_M-1To5_HT-400to600_TuneCUETP8M1_13TeV-madgraphMLM-pythia8	65.9
	DYJetsToLL_M-1To5_HT-600toInf_TuneCUETP8M1_13TeV-madgraphMLM-pythia8	16.72
	DYJetsToLL_M-5to50_HT-70to100_TuneCUETP8M1_13TeV-madgraphMLM-pythia8	301.0
	DYJetsToLL_M-5to50_HT-100to200_TuneCUETP8M1_13TeV-madgraphMLM-pythia8	224.4
	DYJetsToLL_M-5to50_HT-200to400_TuneCUETP8M1_13TeV-madgraphMLM-pythia8	37.87
	DYJetsToLL_M-5to50_HT-400to600_TuneCUETP8M1_13TeV-madgraphMLM-pythia8	3.628
	DYJetsToLL_M-5to50_HT-600toInf_TuneCUETP8M1_13TeV-madgraphMLM-pythia8	1.107
	DYJetsToLL_M-50_HT-70to100_TuneCUETP8M1_13TeV-madgraphMLM-pythia8	169.9
	DYJetsToLL_M-50_HT-100to200_TuneCUETP8M1_13TeV-madgraphMLM-pythia8	147.4
	DYJetsToLL_M-50_HT-200to400_TuneCUETP8M1_13TeV-madgraphMLM-pythia8	40.99
	DYJetsToLL_M-50_HT-400to600_TuneCUETP8M1_13TeV-madgraphMLM-pythia8	5.678
	DYJetsToLL_M-50_HT-600to800_TuneCUETP8M1_13TeV-madgraphMLM-pythia8	1.367
	DYJetsToLL_M-50_HT-800to1200_TuneCUETP8M1_13TeV-madgraphMLM-pythia8	0.6304
	DYJetsToLL_M-50_HT-1200to2500_TuneCUETP8M1_13TeV-madgraphMLM-pythia8	0.1514
	DYJetsToLL_M-50_HT-2500toInf_TuneCUETP8M1_13TeV-madgraphMLM-pythia8	0.003565
	DYJetsToQQ_HT180_13TeV-madgraphMLM-pythia8	1208

Physics process	Dataset name	σ (pb)
$t\bar{t}$	TTJets_Dilept_TuneCUETP8M2T4_13TeV-amcatnloFXFX-pythia8	87.315
Single-top	ST_s-channel_4f_leptonDecays_13TeV-amcatnlo-pythia8_TuneCUETpM1	3.36
	ST_t-channel_antitop_4f_inclusiveDecays_13TeV-powhegV2-madspin-pythia8-TuneCUETP8M1	26.38
	ST_t-channel_top_4f_inclusiveDecays_13TeV-powhegV2-madspin-pythia8_TuneCUETP8M1	44.33
	ST_tW_top_5f_inclusiveDecays_13TeV-powheg-pythia8_TuneCUETP8M1_8ddVersion8	35.85
	ST_tW_antitop_5f_inclusiveDecays_13TeV-powheg-pythia8_TuneCUETP8M1_8ddVersion8	35.83
Di-Boson WW	WW_TuneCUETP8M1_13TeV-pythia8	118.7
Di-Boson WZ	WZ_TuneCUETP8M1_13TeV-pythia8	47.13
Di-Boson ZZ	ZZ_TuneCUETP8M1_13TeV-pythia8	16.523
QCD	QCD_HT100to200_TuneCUETP8M1_13TeV-madgraphMLM-pythia8	27990000
	QCD_HT200to300_TuneCUETP8M1_13TeV-madgraphMLM-pythia8	1712000
	QCD_HT300to500_TuneCUETP8M1_13TeV-madgraphMLM-pythia8	347700
	QCD_HT500to700_TuneCUETP8M1_13TeV-madgraphMLM-pythia8	32100
	QCD_HT700to1000_TuneCUETP8M1_13TeV-madgraphMLM-pythia8	6831
	QCD_HT1000to1500_TuneCUETP8M1_13TeV-madgraphMLM-pythia8	1207
	QCD_HT1500to2000_TuneCUETP8M1_13TeV-madgraphMLM-pythia8	119.9
	QCD_HT2000toInf_TuneCUETP8M1_13TeV-madgraphMLM-pythia8	25.24
Z-Jets	ZJetsToQQ_HT600toInf_13TeV-madgraph	581.9

Boosted Di-tau Reconstruction

- For $\tau_h \tau_h$ final state, the taus are taken from the "slimmedTausBoosted" collection
  - Reconstructed by a version of HPS algorithm that takes two sub-jets from a large-radius jet. (TAU-16-003)
- Due to boosted topology, τ_e or τ_μ could be inside the jet cone for seeding
  → Leads to $\tau_{e/\mu}\tau_h$ being reconstructed as one τ_h
- τ_h in semi-leptonic final state are reconstructed by a modified HPS algorithm
- Removal of electrons and muons from jets. The cleaned jets are then used as seeds for tau reconstruction
  - Electrons and muons are also removed from tau isolation cones

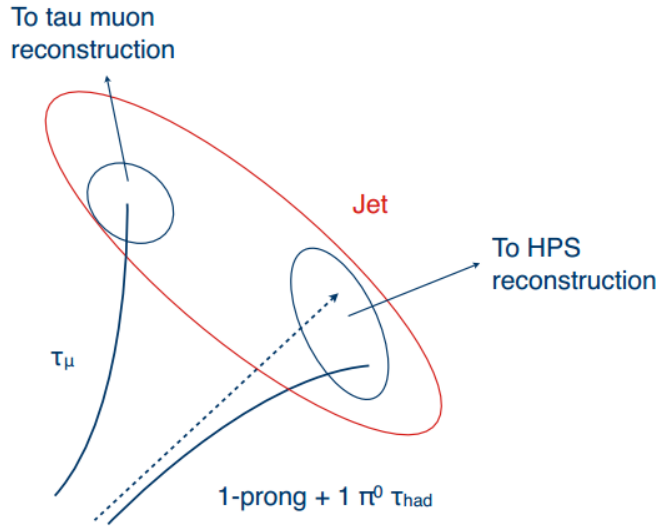

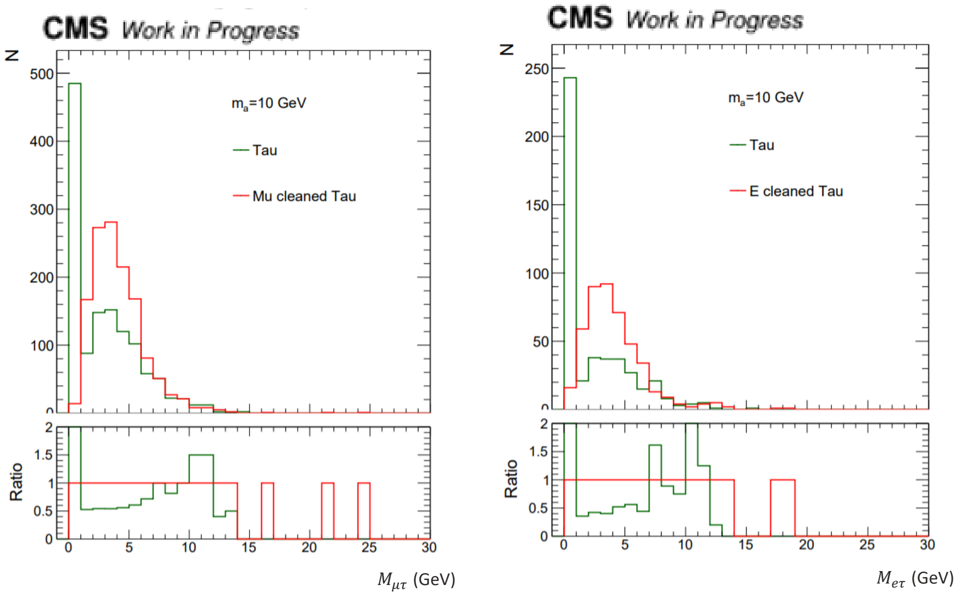

HIG-18-024

Di-tau Opening Angle

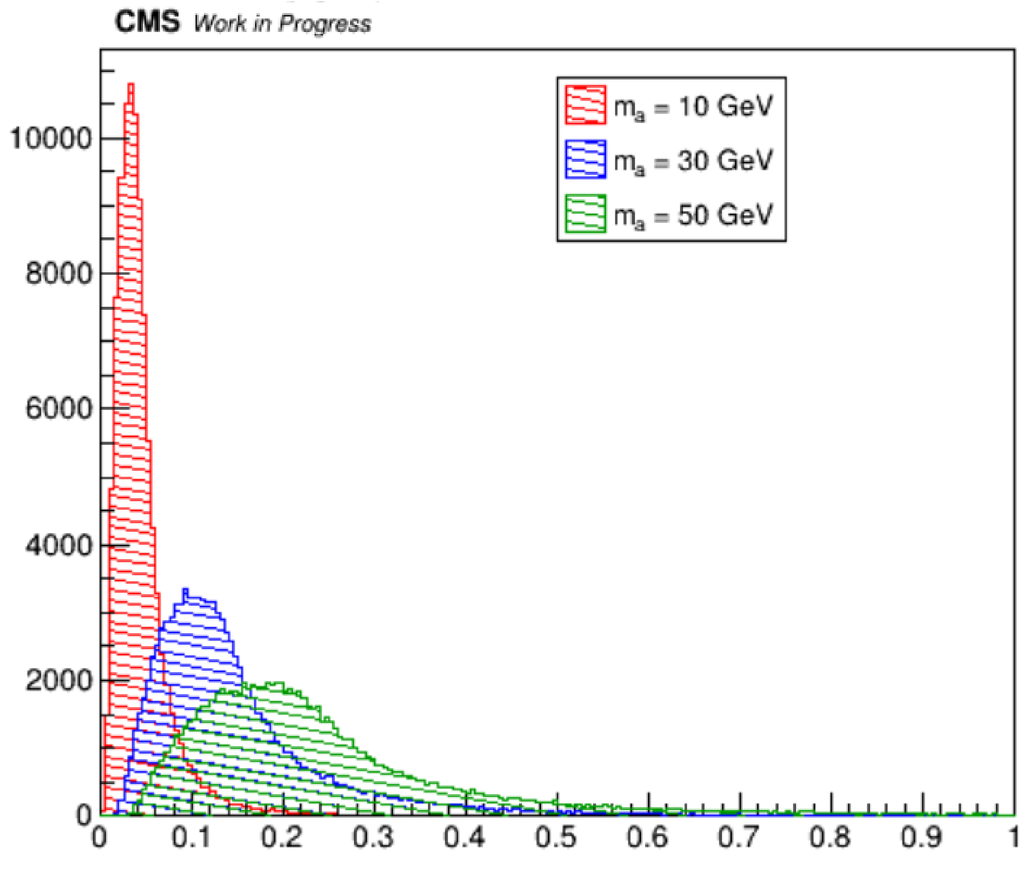

Opening angle (rad)

Mean

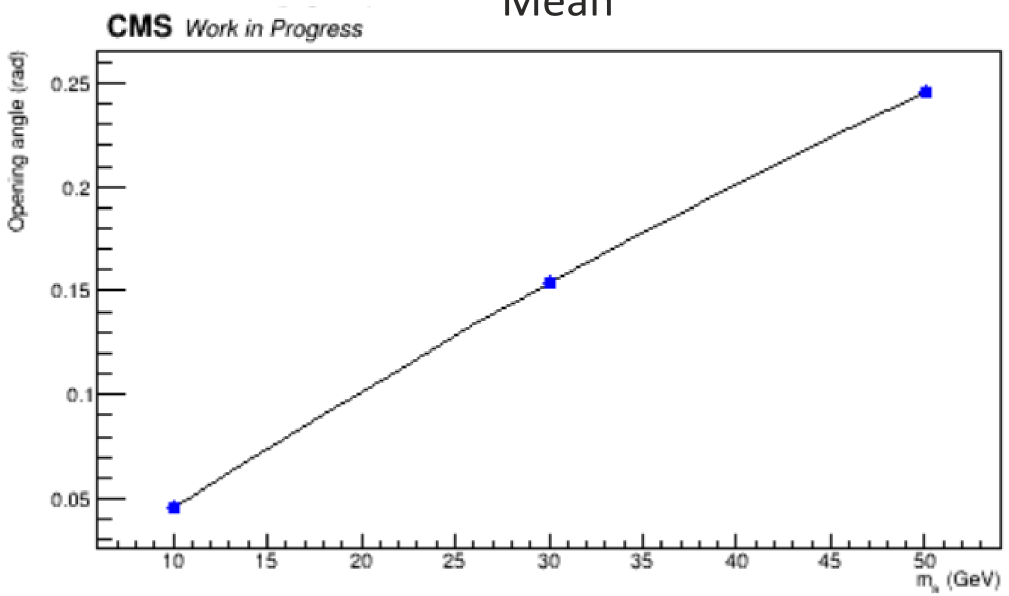

Main Discriminator – ΔR

TCP

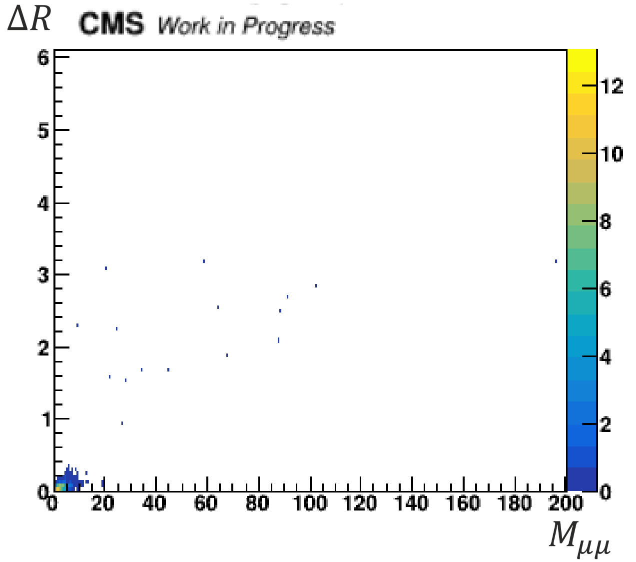

Diboson

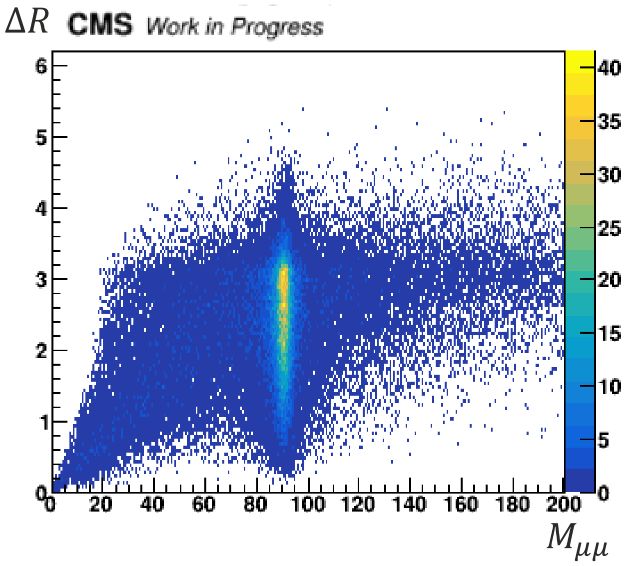

DYJetstoLL

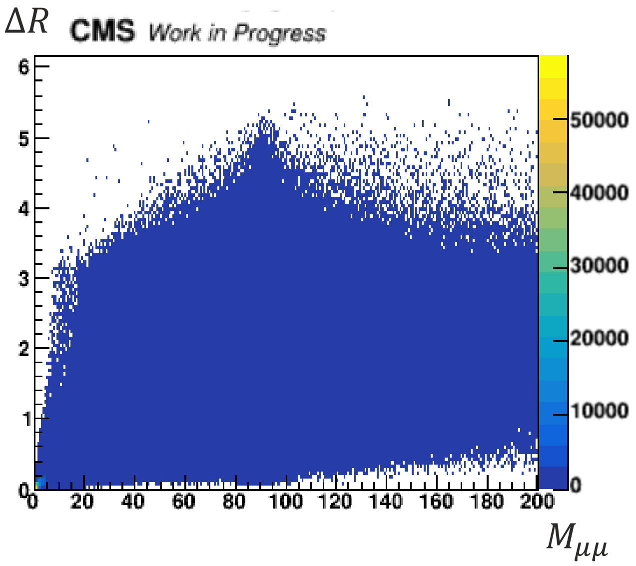

ST

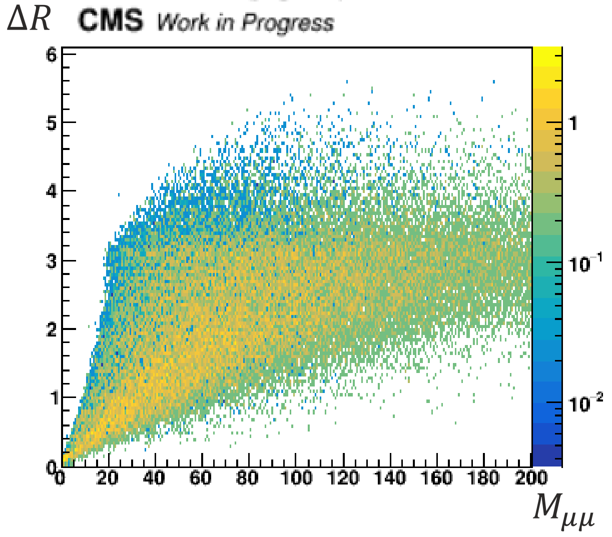

TTJets

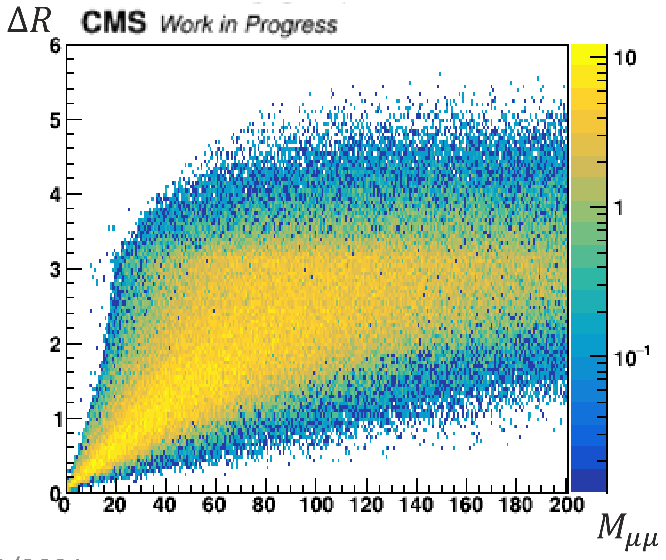

Main Discriminator – Missing E_T

TCP

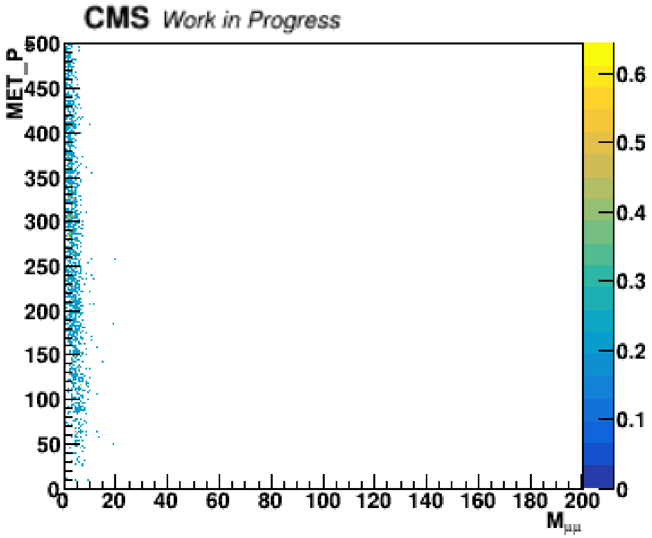

Diboson

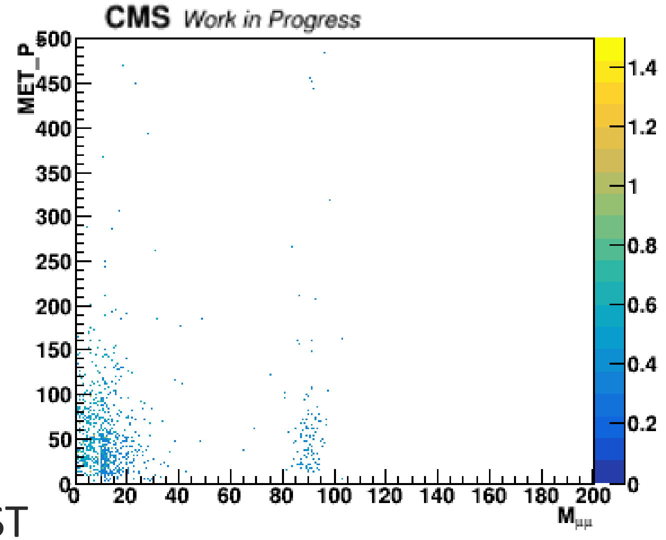

DYJetstoLL

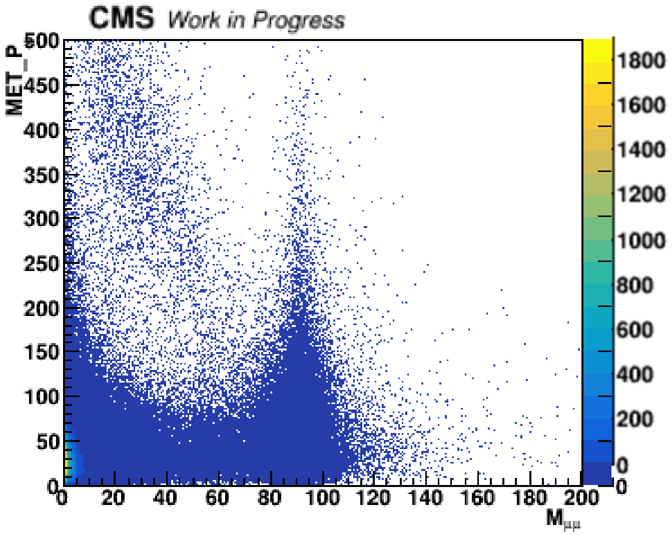

ST

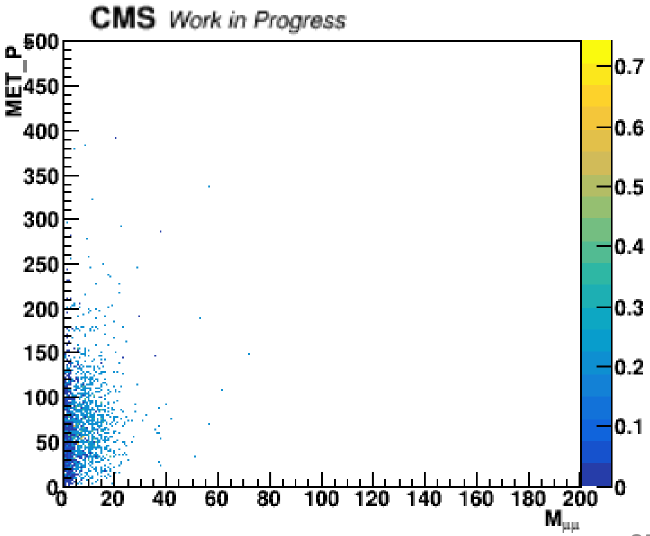

TTJets

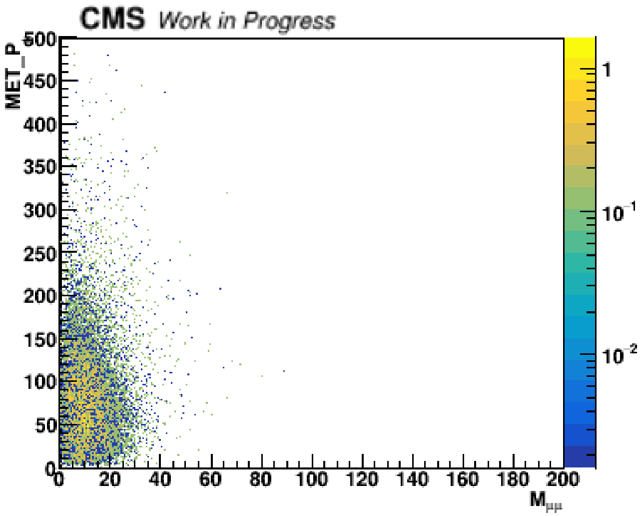

$\Delta\phi$ MET, lMu, Jet

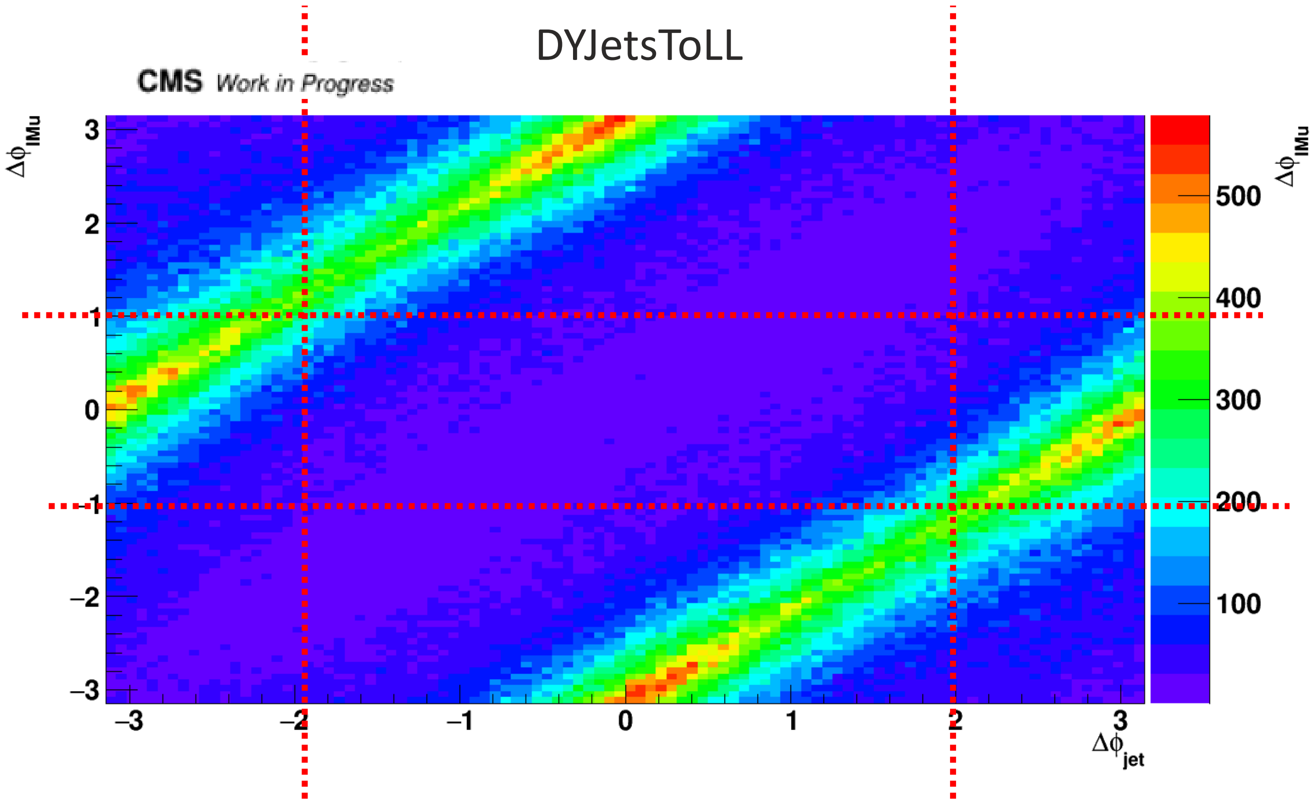

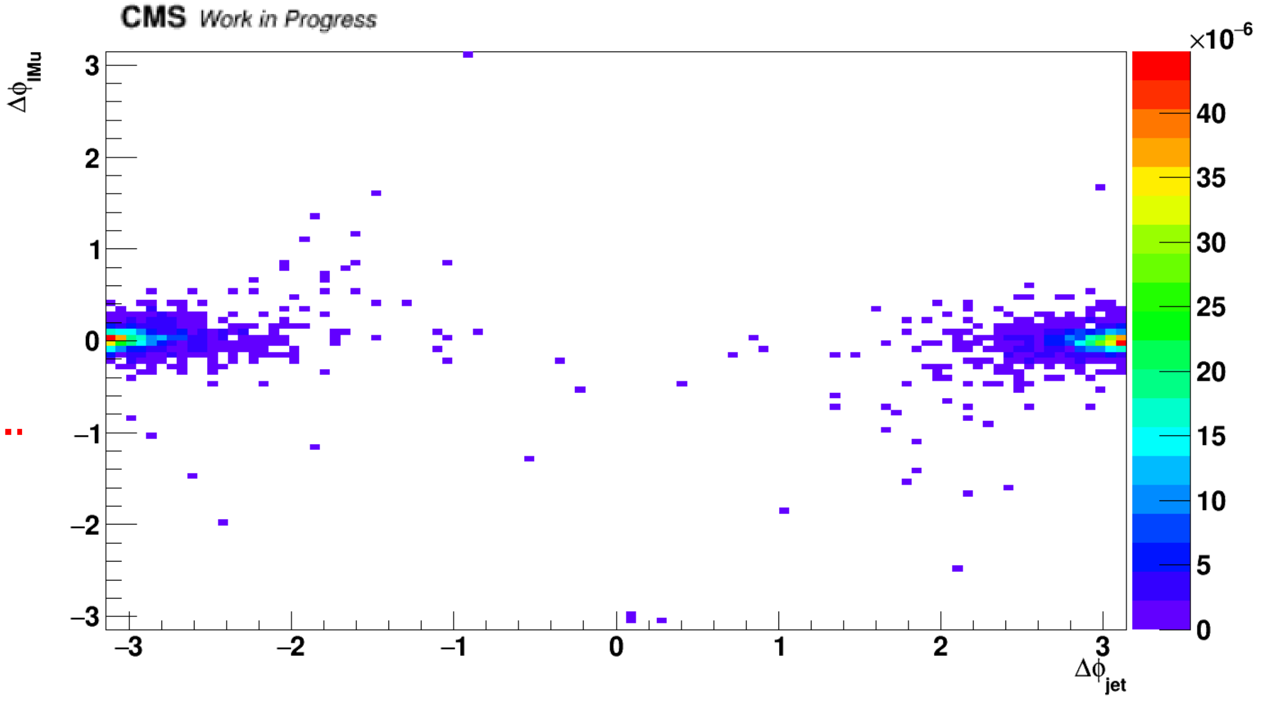

cut $|\Delta\phi_{MET,jet}| > 2$ and $|\Delta\phi_{MET,lMu}| < 1$

Generator Level Electron Pt Distribution in $\tau_e\tau_h$ Final State

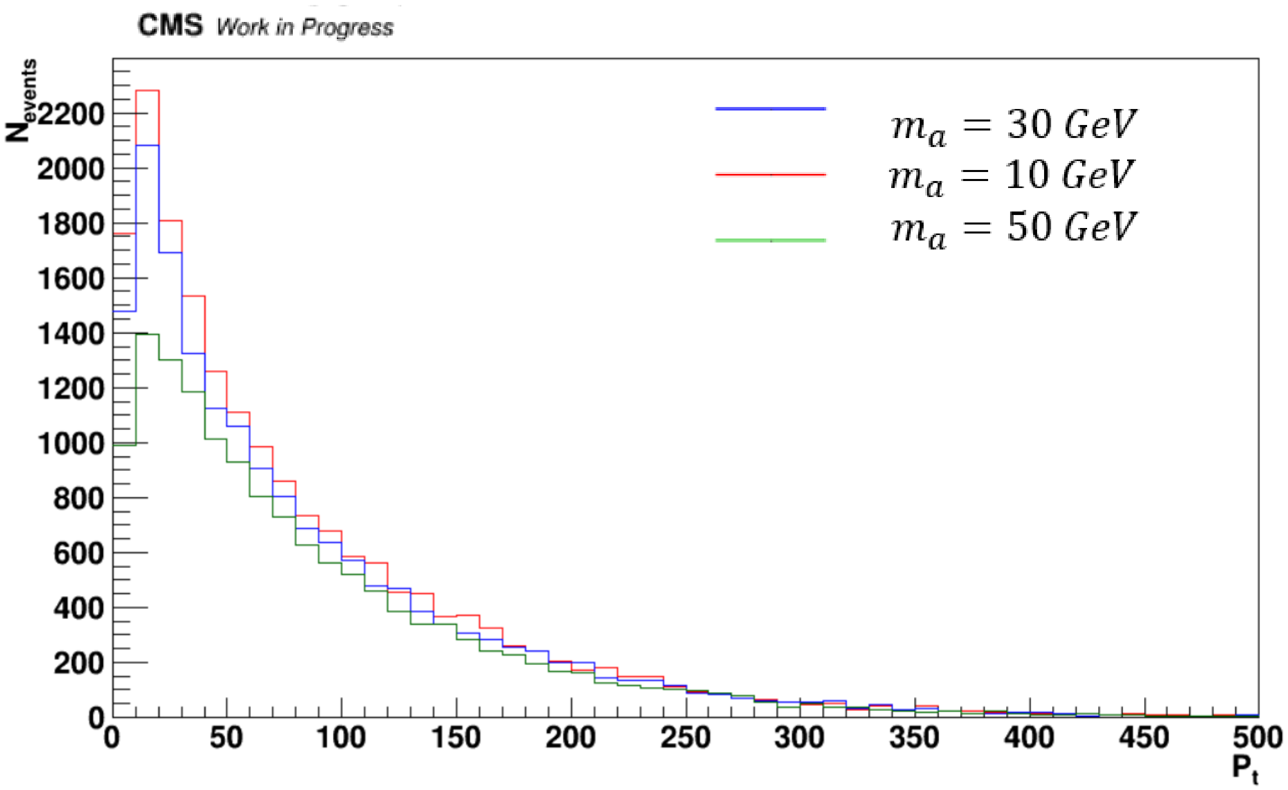

Comparison Between low-pt Electron Reco and Standard Electron Reco

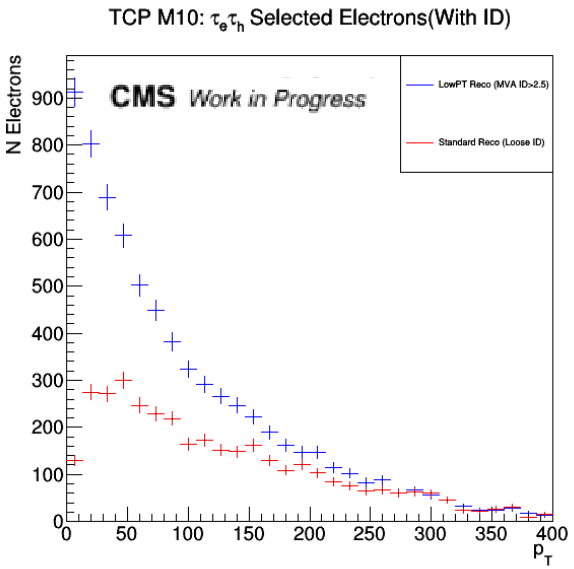

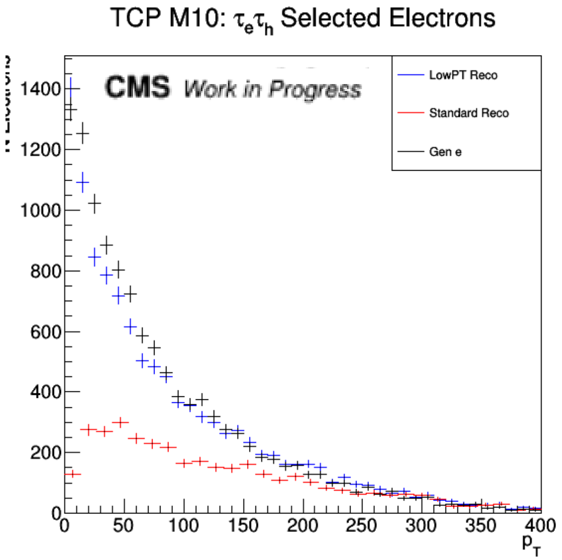

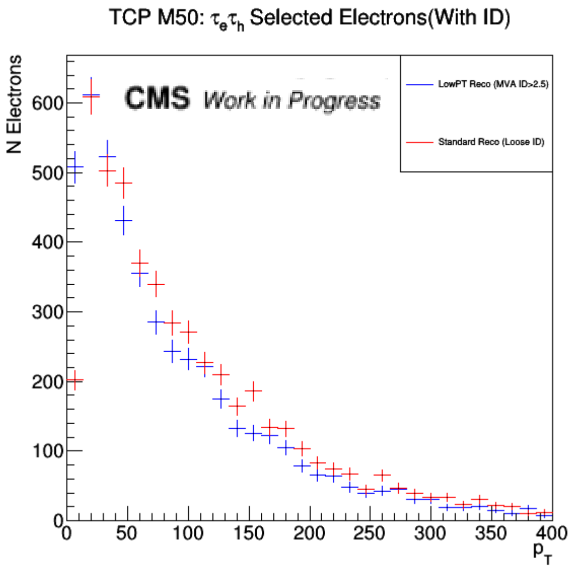

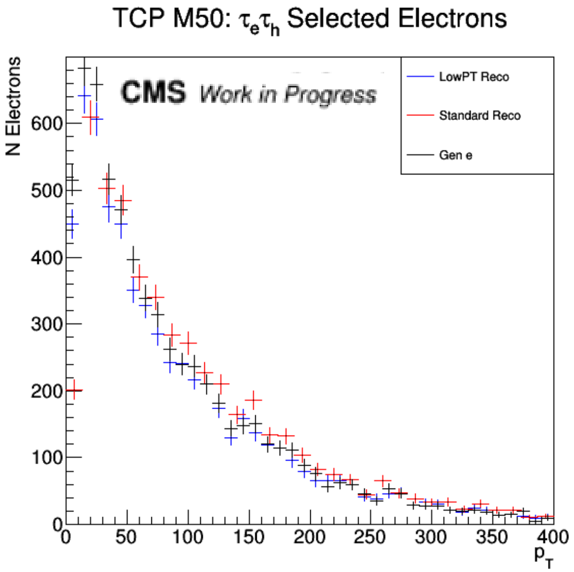

$\tau_h \tau_h$ QCD Background Estimation

All regions have both τs not passing VLoose discriminant

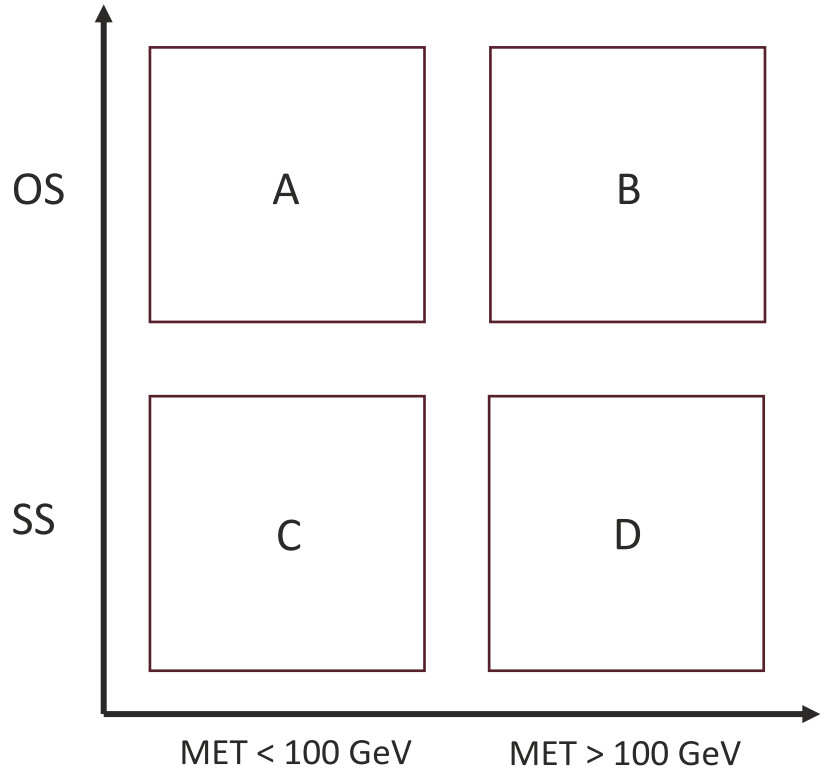

MET Pt Distribution on QCD

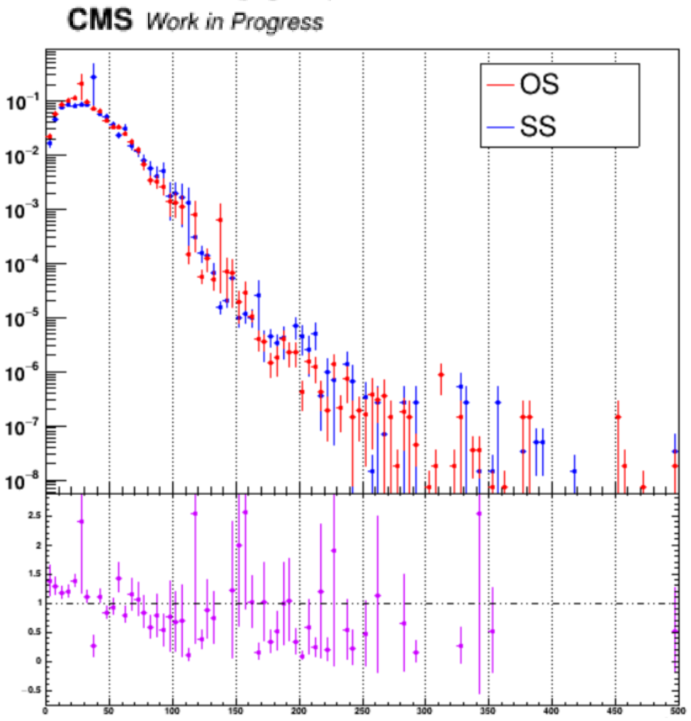

The ratio of the distribution of MET Pt is somewhat close to 1

Visible mass plots

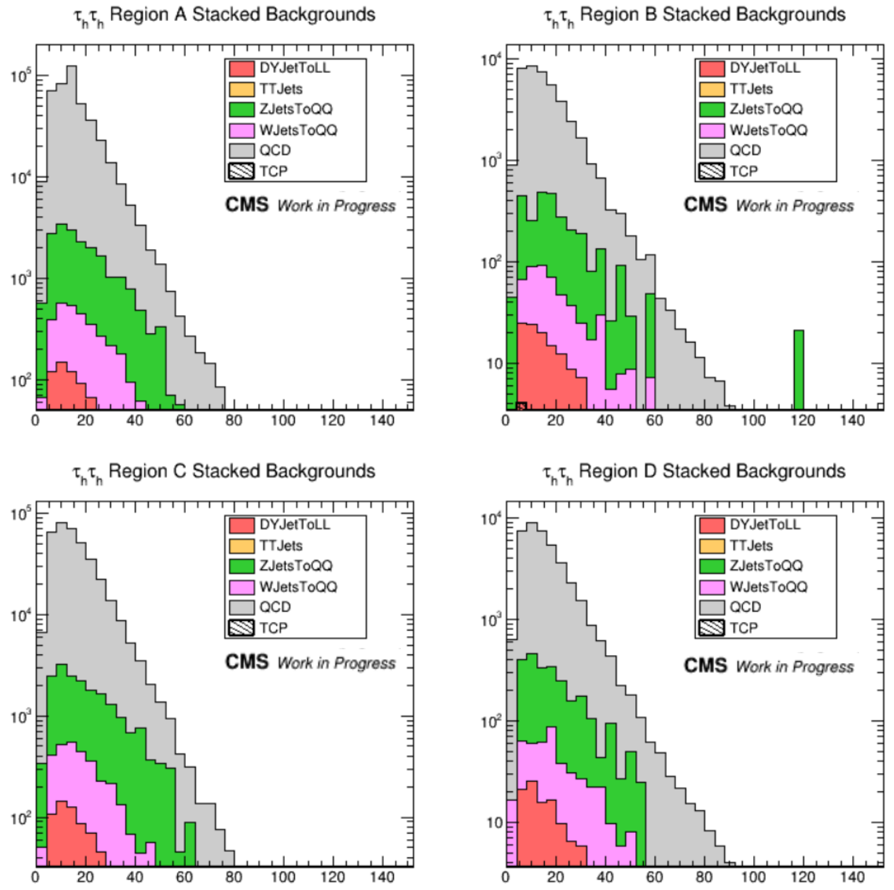

Regions dominated by backgrounds

$\tau_h\tau_h$ QCD Background Estimation

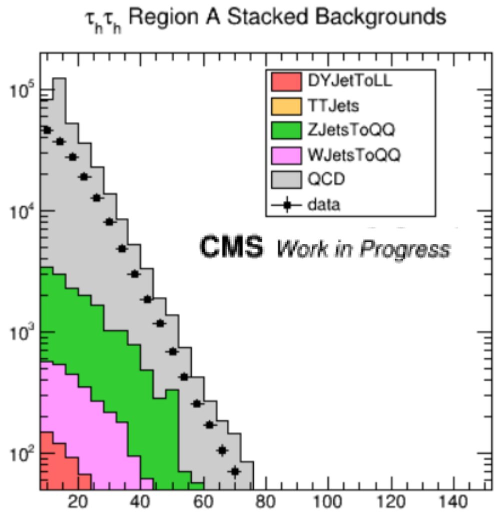

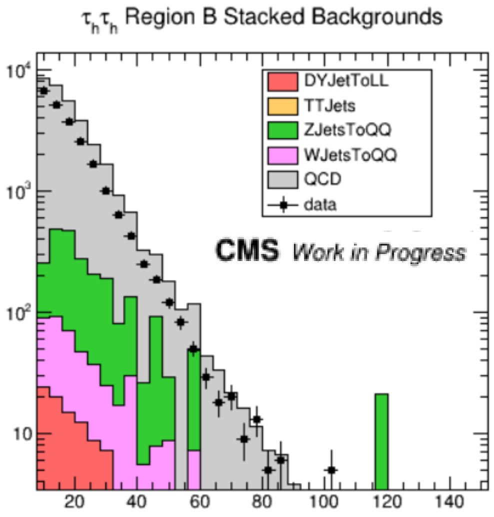

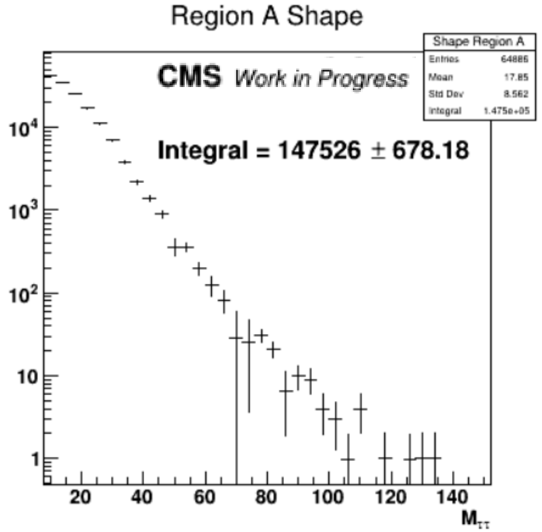

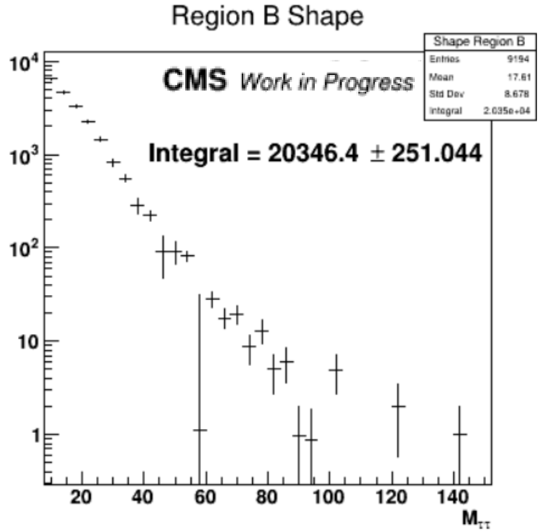

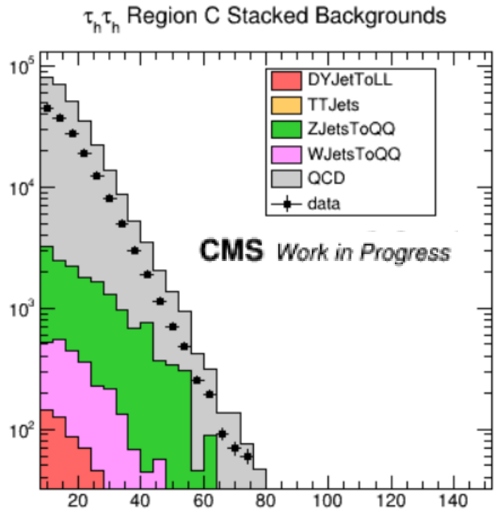

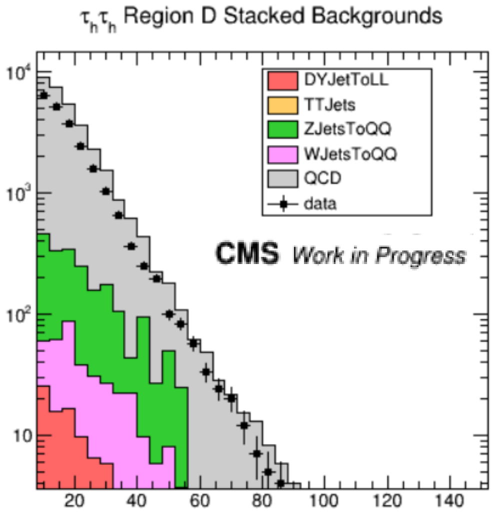

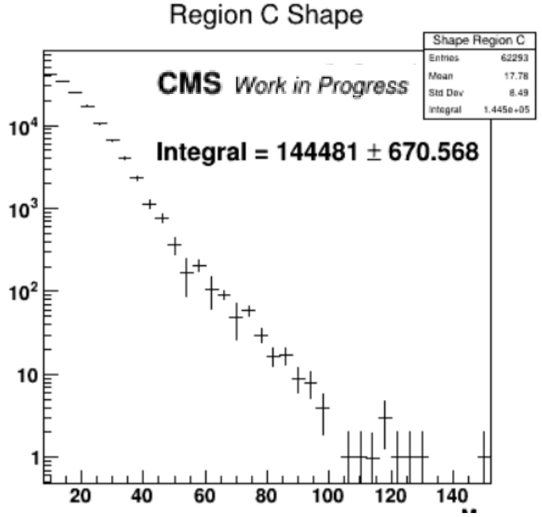

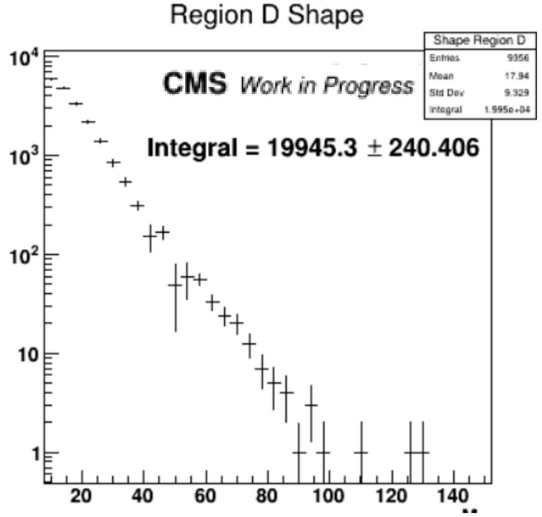

$\tau_h \tau_h$ QCD Background Estimation

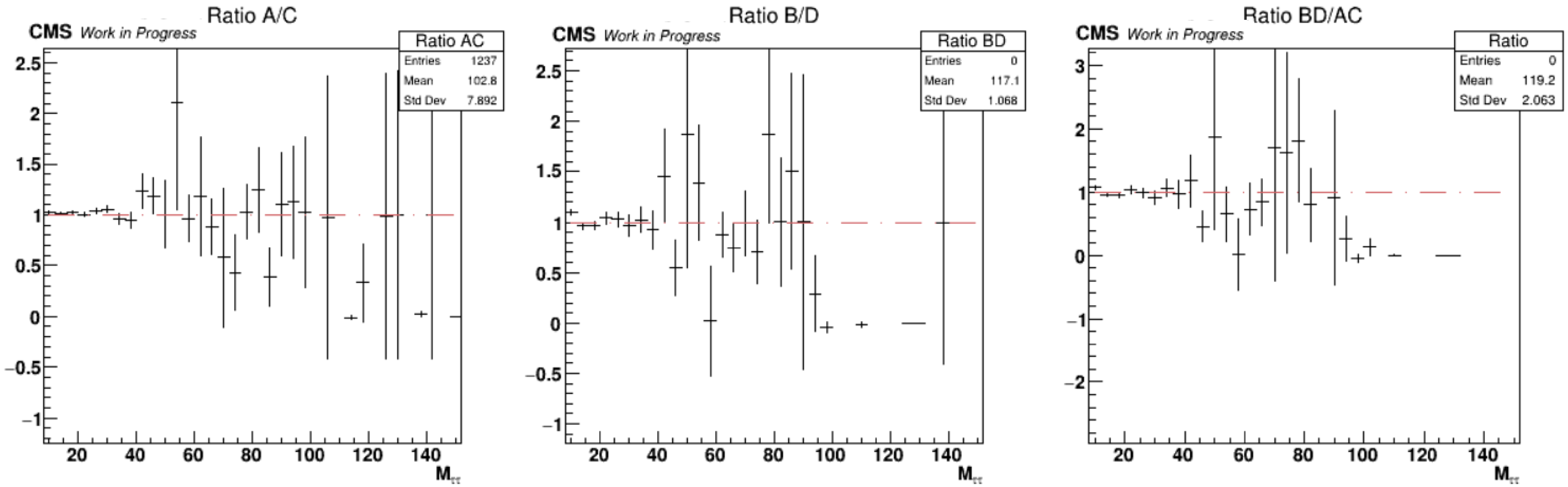

	Integral	Ratio	
Region A	147526±678.18	$\frac{A}{C}$	1.02108±0.00502
Region C	144481±670.568		
Region B	20346.4±251.044	$\frac{B}{D}$	1.02011±0.0358
Region D	19945.3±240.406		

$$A = C \times \frac{B}{D} = 14772.2 \pm 858.305$$

$$B = D \times \frac{A}{C} = 20365.7 \pm 265.108$$

$\tau_h \tau_h$ QCD Background Estimation

Scale data on Region C by 1.02011

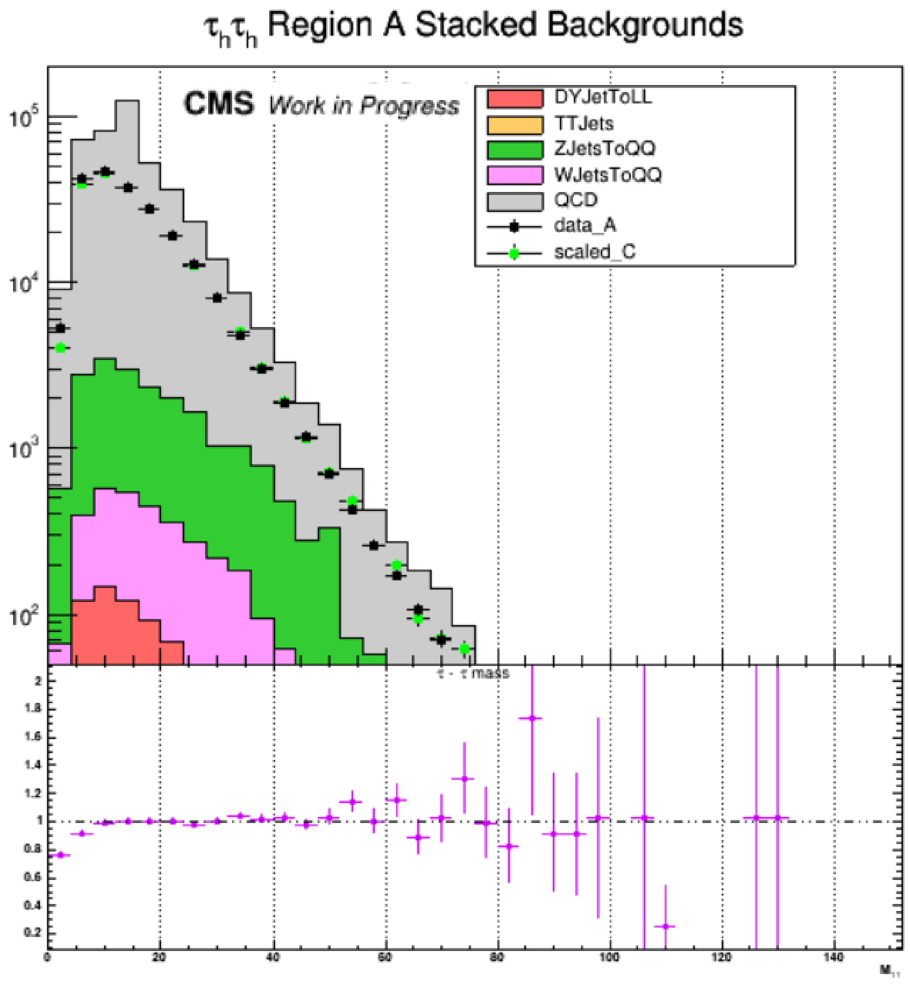

Scale data on Region D by 1.02108

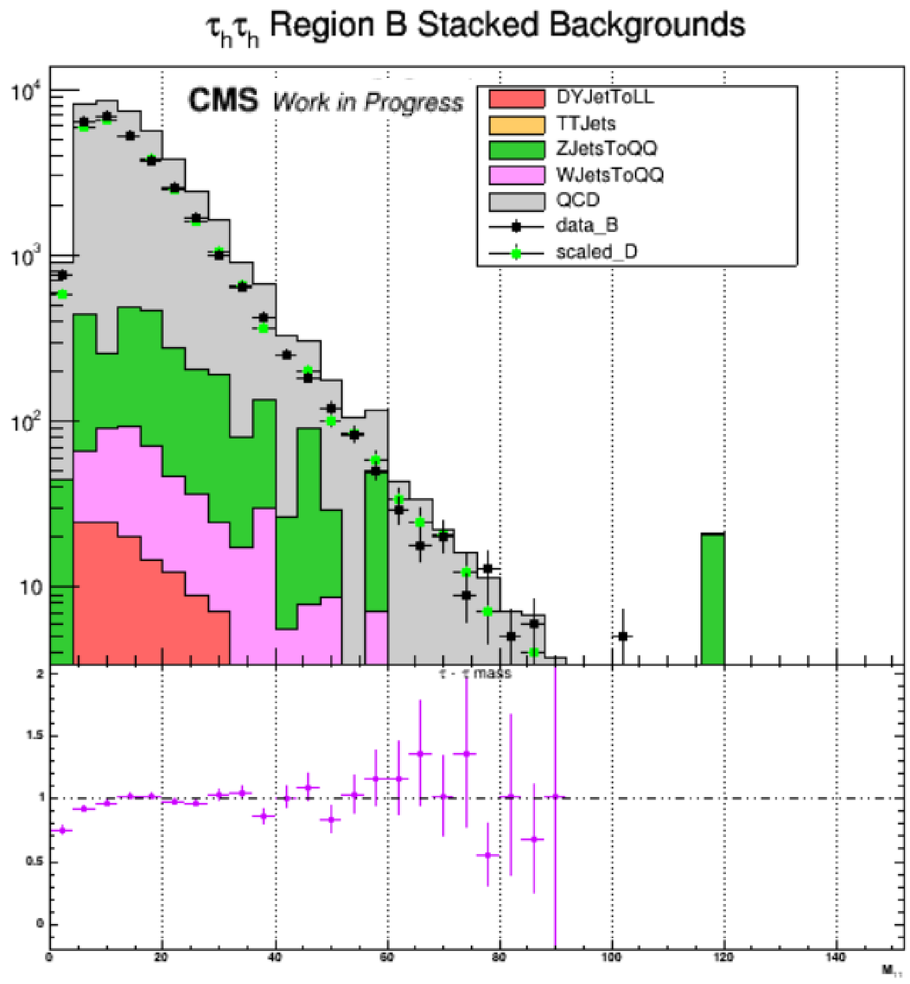

Trigger Efficiency as a Function of the ISR jet Pt

The triggers we use are:

Jet Trigger: HLT_PFJet450

HLT_PFHT900

HLT_CaloJet500_NoJetID

Muon Trigger: HLT_IsoTkMu24

HLT_IsoMu24

HLT_TKMu50

HLT_Mu50

The jet trigger is fully efficient above 500 GeV and adding Muon triggers help recover some of the efficiency at low jet pT.